

# Conformational Analysis of Fluoro-, Chloro-, and Proteo-alkene Gly-Pro and Pro-Pro Isosteres to Mimic Collagen

Paul J. Arcoria, Rachel I. Ware, Sunny V. Makwana, Diego Troya, Felicia A. Etzkorn\*

Department of Chemistry, Virginia Tech, Blacksburg VA, 24061, United States

\*Email: fetzkorn@vt.edu

**Abstract:** Collagen is the most abundant human protein, with the canonical sequence (Gly-Pro-Hyp)<sub>n</sub> in its triple helix region. Cis-trans isomerization of the Xaa-Pro amide has made two of these amide bonds the target of alkene replacement: the Gly-Pro and the Pro-Hyp positions. The conformations of Gly-Pro and Pro-Pro (as a Pro-Hyp model) fluoro-, chloro- and proteo-alkene mimic models were investigated computationally to determine whether these alkenes can stabilize the polyproline type II (PPII) conformation of collagen. MP2 calculations with various basis sets were used to perform the conformational analyses and locate stationary points. The calculation results predict that fluoro- and chloro-alkene mimics of Gly-Pro and Pro-Pro can participate in  $n \rightarrow \pi^*$  donation to stabilize PPII conformations, yet they are poor  $n \rightarrow \pi^*$  acceptors, shifting the global minima away from PPII conformations. For the proteo-alkene mimics, the lack of significant  $n \rightarrow \pi^*$  interactions and unstable PPII-like geometries explains their known destabilization of the triple helix in collagen-like peptides.

## Introduction

Collagen is one of the most important structural proteins in vertebrates, accounting for 30% of all vertebrate protein.<sup>1</sup> It consists of three left-handed poly-proline type II (PPII) helices that

intertwine around a common screw axis to form the right-handed triple helix.<sup>2, 3</sup> PPII helices are a frequently occurring protein secondary structure that are prevalent in fibrillar proteins.<sup>4</sup> They serve key roles in signal transduction and protein complex assembly.<sup>4</sup> The three PPII helices of collagen exist as repeating polymers of (Gly–Xaa–Yaa)<sub>n</sub>, in which 25% of all Xaa residues are (2*S*)-proline (Pro) and 38% of all Yaa residues are (2*S*,4*R*)-hydroxyproline (Hyp).<sup>1</sup> This makes Gly–Pro–Hyp the most common sequence of the triple helix.<sup>5</sup> Gly–Pro–Pro collagen-like peptides have been frequently used in studies of the triple helix.<sup>6</sup>

The tertiary amide of the Xaa–Pro motif has an unusually high proportion of the *cis* isomer due to steric destabilization of the *trans* isomer.<sup>7</sup> While over 99% of secondary amides adopt the *trans* conformation, 10–30% of Xaa–Pro tertiary amides in peptides and unfolded proteins appear as the *cis* conformation.<sup>8</sup> Propagation of the collagen triple helix is rate-limited by the isomerization of the Xaa–Pro motif.<sup>9</sup>

Due to the high degree of *sp*<sup>2</sup>-character of amides, alkenes have proven to be excellent mimics of prolyl amides.<sup>10-12</sup> However, we have previously shown that converting an Xaa–Pro amide to an alkene decreases the stability of the triple helix.<sup>13, 14</sup> Substitution of a single Gly–Pro peptide per strand with an alkene in a 27-residue collagen-like peptide leads to a change in the folding temperature of  $\Delta T_m = -21.7$  °C compared to the native collagen-like peptide control.<sup>13</sup> Replacement of a Pro–Pro amide, with concomitant loss of an interstrand hydrogen bond, was even more disruptive to triple helix folding with a change in folding temperature of  $\Delta T_m = -53.6$  °C compared to the native control.<sup>14</sup> This showed that the entropic reduction afforded by the olefin mimic does not compensate for some missing interactions that are intrinsic to the peptide bond. The destabilization with the proteo-alkene mimics could be caused by the loss of noncovalent interactions that may be present with the native amide in the collagen triple helix.

Raines and coworkers have shown, computationally and experimentally, that collagen is stabilized by a series of electronic  $n \rightarrow \pi^*$  interactions.<sup>7, 15</sup> In the trans conformation of Xaa-Pro models, a lone pair of Xaa  $C_i=O$  delocalizes into the Pro  $C_{i+1}=O$   $\pi^*$  anti-bonding orbital.<sup>7, 16</sup> Electron delocalization follows the Bürgi-Dunitz trajectory of nucleophilic addition to a carbonyl, in which the angle of approach ( $\tau_{BD}$ :  $\angle O_i \cdots C_{i+1}=O$ ) is approximately  $109^\circ$ , and the distance between the donor oxygen and acceptor carbon ( $\delta_{BD}$ ) is within the sum of their respective van der Waals radii (Figure 1).<sup>17</sup> Donation into the  $\pi^*$  orbital also produces slight  $sp^3$  character in the acceptor  $C_{i+1}$  atom resulting in pyramidalization, as measured by the angle  $\theta_{BD}$ .<sup>18</sup> Carbonyl pyramidalization is a signature of the  $n \rightarrow \pi^*$  interaction, and the mean  $\theta_{BD}$  angle in  $\alpha$ -helices has been reported as  $+4^\circ \pm 1.1^\circ$ .<sup>18</sup> In  $\alpha$ -helices, nearly every carbonyl acts as both an  $n \rightarrow \pi^*$  donor and acceptor.<sup>15</sup> A density functional theory calculation estimated that the  $n \rightarrow \pi^*$  interaction of Ac-Pro-NMe<sub>2</sub> contributes approximately 0.14 (*C $\gamma$ -endo*) or 0.53 kcal/mol (*C $\gamma$ -exo*) of stability, and the weighted average was estimated at 0.27 kcal/mol.<sup>19</sup> However, evidence of the  $n \rightarrow \pi^*$  interaction is lacking in the <sup>13</sup>C=O NMR chemical shifts of proteins.<sup>20</sup>

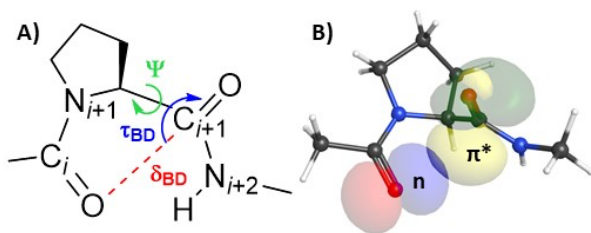


**Figure 1.** **A)** Bürgi-Dunitz trajectory angle ( $\tau_{BD}$ ) and distance ( $\delta_{BD}$ ) of the oxygen lone-pair donor ( $n$ ) with the carbonyl acceptor ( $\pi^*$ ) of the subsequent amide bond describes an  $n \rightarrow \pi^*$  interaction found in collagen. The torsion angle varied for the calculations is  $\Psi$ . **B)** Calculated NBOs showing the overlap of oxygen non-bonding orbital (blue/red) and  $C'_{i+1}=O$  antibonding  $\pi^*$  orbital

(yellow/green).<sup>16</sup>

In a recent paper, we reported the conformational variation in stability of small PPII models of the amide-amide interactions. We found forward and reverse, re- and si-face, and reciprocal  $n \rightarrow \pi^*$  interactions,<sup>21</sup> and hydrogen bonds that stabilize PPII or competing conformations.<sup>16</sup> We calculated the relative energies of these minima and the barriers between them, as well as the second-order perturbation energies (E2PERT) from Natural Bond Orbital (NBO) calculations of the  $n \rightarrow \pi^*$  and hydrogen-bonded interactions.<sup>16</sup> For the Gly–Pro–Pro (GPP) model, the global minimum shows an  $n \rightarrow \pi^*$  interaction that stabilizes the PPII conformation.<sup>16</sup> For the Pro–Pro–Gly (PPG) model, the global minimum involves a hydrogen bond between the Pro<sub>*i*+1</sub> N and the Gly<sub>*i*+2</sub> NH that is conformationally distinct from the PPII conformation, though only 1.0 kcal/mole more stable.<sup>16</sup> The Pro–Gly–Pro (PGP) model was shown to be quite conformationally flexible with multiple minima due to the lack of a restricted  $\Phi$ -bond in Gly.<sup>16</sup>

Due to their rigidity and hydrolytic stability, fluoro- and chloro-alkenes have found use in medicinal chemistry as peptide-bond bioisosteres.<sup>22, 23</sup> The similar sizes of fluorine and oxygen atoms (van der Waals radii = 1.47 Å and 1.52 Å, respectively),<sup>24</sup> and the similar bond lengths of C=O (1.2 Å) and C–F (1.4 Å), allow for analogous pseudo-1,3-allylic strain.<sup>25</sup> However, since fluorine is smaller and more electronegative than oxygen (EN = 3.98 and 3.44, respectively),<sup>26</sup>  $n \rightarrow \pi^*$  donation by the fluoro-alkene may be less prevalent. Kamer et al. found crystallographic evidence of  $n \rightarrow \pi^*$  interactions of halides (F, Cl, Br, and I) with amide carbonyls.<sup>27</sup> Jakobsche et al. have shown experimentally that a Pro–Gly alkene isostere is a poor  $n \rightarrow \pi^*$  acceptor due to Pauli repulsion with the  $\pi$ -cloud, while a similar fluoro-alkene reduces  $n \rightarrow \pi^*$  Pauli repulsion.<sup>28</sup> Replacement of the OH of Hyp with the analogous stereoisomer, 4(*R*)-fluoroproline, significantly stabilizes the collagen triple helix.<sup>29</sup> We are curious to see if the Gly–Pro and Pro–Pro fluoro-

alkene isosteres might similarly enhance the stability of the collagen triple helix.

The atomic radius of chlorine (1.75 Å) and the C–Cl bond length (1.72 Å)<sup>24</sup> are expected to have a deleterious effect on the pseudo-1,3-allylic strain and interstrand packing of a chloro-alkene mimic. Chloro-alkenes may also suffer as  $n \rightarrow \pi^*$  acceptors due to Pauli repulsion.<sup>28</sup> However, the larger 3<sup>rd</sup> row lone pairs and lower electronegativity of chlorine (EN = 3.16)<sup>26</sup> may provide more overlap and stronger  $n \rightarrow \pi^*$  donation. It would be interesting to see how a chloro-alkene mimic might be accommodated in a collagen triple helix. Chlorine was substituted as 4(*R*)-chloroproline (Clp) for the side-chain OH in Hyp.<sup>30</sup>

In this work, we calculate the impacts of fluoro-, chloro-, and proteo-alkene mimics of Gly–Pro and Pro–Pro on the conformation of the PPII helix found in collagen. While the relatively small models of this work cannot capture the extent of all non-bonded interactions within a full triple helix, our intention was to closely examine very local interactions that contribute to the PPII-like conformation with high-level *ab initio* calculations. The calculations herein help us to predict the potential of fluoro- and chloro-alkenes to stabilize collagen-like peptides, and to understand the failure of the simple proteo-alkene mimics to stabilize the collagen conformation.<sup>13, 14</sup> Substituting halogenated alkenes, i.e. a fluoro- or chloro-alkene, may provide non-covalent interactions that would allow them to adopt the PPII-like conformation,<sup>15, 31, 32</sup> while still reducing the entropic cost of cis-trans proline isomerization in folding.<sup>9</sup>

## Computational Methods

Preliminary geometries were obtained from residues Hyp20–Gly21–Pro22–Hyp23–Gly24 of the collagen triple helix high-resolution crystal structure 1CAG of Bella et al.<sup>33</sup> and modified to the highlighted portions shown in Figure 2. (4*S*)-Hydroxyproline was changed to L-proline to reduce

the number of heavy atoms in the calculations. Initial optimizations were conducted using Gaussian 09 in WebMO at the second-order Møller-Plesset (MP2) level of theory with the 6-31+G(d) basis set, including the solvent effects of water by the polarizable continuum model.<sup>34, 35</sup> Diffuse functions on heavy atoms were incorporated to capture delocalization of electron density that is a signature of  $n \rightarrow \pi^*$  interactions.<sup>36</sup> Coordinate scans allowed for optimization of all degrees of freedom except for the  $\Psi$  dihedral angle being rotated.

For the G(-X)=PP  $n \rightarrow \pi^*$  donor and GP(-X)=P  $n \rightarrow \pi^*$  acceptor models, where X = F, Cl, or H, scans of the  $\Psi$  dihedral angle were conducted from  $+170^\circ$  to  $-180^\circ$  in  $10^\circ$  increments. For the P(-X)=PG  $n \rightarrow \pi^*$  donor and PG(-X)=P  $n \rightarrow \pi^*$  acceptor models, scans of the  $\Psi$  dihedral angle were performed from  $-170^\circ$  to  $+180^\circ$  in  $10^\circ$  increments. For the PG(-X)=P scans, the  $\Phi$  dihedral angle ( $C'_i-N_{i+1}-C\alpha_{i+1}-C'_{i+1}$ ) was also fixed to  $-72^\circ$ , the  $\Phi$  angle found in collagen-like peptides,<sup>33</sup> and the remaining coordinates were fully optimized. The energy of the global minimum structure in each model series was normalized to 0.0 kcal/mol.

The two lowest-energy minima found in each of the 12 models were fully optimized at the MP2/6-31+G(d) level, then optimized further at the MP2/6-311+G(2d,p) level (Tables 1, 2, S1, S2). Single point energies of the unrestrained MP2/6-31+G(d) geometries were also calculated at the MP2/6-311+G(2d,p) level. In all scans, the maxima found closest to the ideal collagen angles were optimized unrestrained at the MP2/6-31+G(d) level, and single point energies of those geometries were calculated at the MP2/6-311+G(2d,p) level. The energy difference between the single point calculations of minima and maxima at MP2/6-311+G(2d,p) was used to estimate the energy of conformational barriers relative to minima optimized at that level (Tables S1, S2).

For minima optimized at the MP2/6-311+G(2d,p) level, the distances between  $C_i-X \cdots C_{i+1}=O$  or

$C_i=O\cdots C_{i+1}-X$  ( $\delta_{BD}$ ), the angles between  $C_i-X\cdots C_{i+1}=O$  or  $C_i=O\cdots C_{i+1}-X$  ( $\tau_{BD}$ ), and the pyramidalization  $\Theta_{BD}$  angle formed between the  $C\alpha_i-C'_i-C/N_{i+1}$  plane and the  $C'_i=O$  vector were determined (Tables 1, 2, S1, S2).<sup>16</sup> In this work,  $\Theta_{BD}$  is positive when the accepting carbon is puckered toward the donating atom. The accepting *re* or *si*  $\pi^*$  face of the carbonyl for PPII-like geometries of Gly–Pro models (Table 1) and Pro–Pro models (Table 2) that were within the Bürgi-Dunitz limits were noted. The energy of orbital interactions was quantified by Natural Bond Order (NBO) second-order perturbation analysis (E2).<sup>37</sup> We consider an absence of orbital overlap when the NBO E2 energy is less than a 0.1 kcal/mol threshold. NBOs were used to visualize orbital interactions.<sup>37</sup> All NBO images have an MO isosurface value of 0.050 with 64,000 grid points. The accepting  $\pi^*$  face and pyramidalization,  $\Theta_{BD}$ , are not reported for those models that do not show significant  $n\rightarrow\pi^*$  overlap. An  $n\rightarrow\pi^*$  donation is expected to occur in donor models when the donating atom is fluorine,  $\delta_{BD} < 3.17$  Å; when the donating atom is chlorine,  $\delta_{BD} < 3.45$ ; when the donating atom is hydrogen,  $\delta_{BD} < 2.90$  Å; and when the donating atom is oxygen,  $\delta_{BD} < 3.22$  Å. The accepting atom is carbon in all cases. Geometric parameters of all minima and maxima of Gly–Pro and Pro–Pro mimic models are given in Tables S1 and S2 respectively.

The average  $\Psi$  and  $\Phi$  dihedral angles (Table S3), were measured using the ‘phi\_psi’ PyMOL function, and the average distance ( $\delta_{BD}$ ), and angles ( $\tau_{BD}$ ) (Table S4) of the high-resolution (1.3 Å) crystal structure of the collagen-like peptide, (Gly–Pro–Pro)<sub>10</sub> (PDB ID: 1K6F) were measured using PyMOL.<sup>6, 38</sup> Amino acids  $\pm 6$  from both ends of each peptide chain were excluded to limit end-effects on our data. The 1K6F crystal structure includes two independent triple helices giving six measurements at each residue position for more robust averages.<sup>6</sup>

All alkene PPII-like minima were superimposed on the appropriate segment of the 1.3 Å collagen-

like peptide crystal structure (PDB ID: 1K6F residues Pro13–Gly14–Pro15–Pro16–Gly17)<sup>6</sup> using Maestro software from Schrödinger, Inc.<sup>39</sup> The root-mean-square deviation (rmsd) between calculated and experimental models were acquired by manual superposition of all heavy atoms, plus the alkene hydrogen for proteo-alkene models (Tables 1, 2).

## Results and Discussion

We designed our models to capture both  $n \rightarrow \pi^*$  donor and  $n \rightarrow \pi^*$  acceptor interactions of the alkenes that would be present at *one* position of a PPII helix using high-level conformational analysis of separate donor and acceptor models for a total of 12 unique models. In a full-length peptide, these mimics would be subject to both types of non-bonded interactions. For each alkene, the  $n \rightarrow \pi^*$  donor and acceptor models must be considered together to predict how that alkene will behave in a triple-helix peptide. Initial models of Gly–Pro and Pro–Pro fluoro-, chloro-, and proteo-alkene isosteres were created as shown in the colored portions of Figure 2.

Replacement of the Gly–Pro amide bond led to the G(–X)=PP model with the alkene X group as an  $n \rightarrow \pi^*$  donor (Figure 2A), and the PG(–X)=P model with the C=C  $\pi^*$  orbital as an  $n \rightarrow \pi^*$  acceptor (Figure 2B). Replacement of the Pro–Pro amide bond led to the P(–X)=PG model with the alkene X group as an  $n \rightarrow \pi^*$  donor (Figure 2C) and the GP(–X)=P model with the C=C  $\pi^*$  orbital as an  $n \rightarrow \pi^*$  acceptor (Figure 2D). In our model numbering scheme, *D* = potential  $n \rightarrow \pi^*$  donor and *A* = potential  $n \rightarrow \pi^*$  acceptor (Table 1). The GPP amide is both the Gly–Pro  $n \rightarrow \pi^*$  donor and Pro–Pro  $n \rightarrow \pi^*$  acceptor, so it is labeled as *D/A* in both cases. Models with a Pro–Gly amide substitution were omitted because they naturally adopt the trans conformation, and collagen would not benefit from this substitution.<sup>40</sup> Substitution of an aza-Gly mimic into collagen, however, was stabilizing.<sup>41</sup>



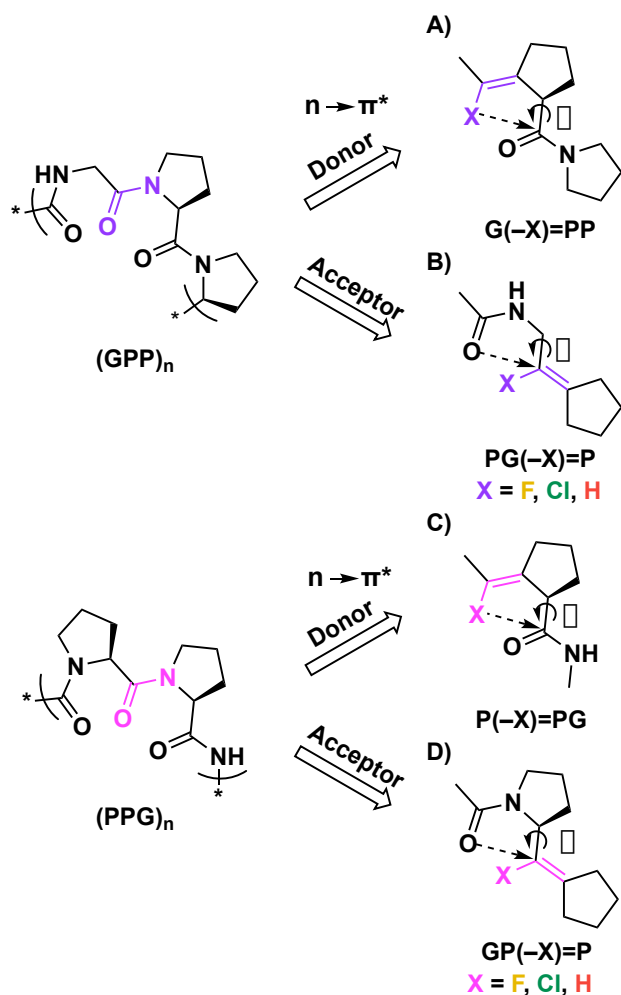


**Figure 2.** Two Xaa-Pro amide bond substitution models: Gly-Pro (top) and Pro-Pro (bottom). **A)** Gly-Pro alkene substitutions are potential  $n \rightarrow \pi^*$  donors to the Pro-Pro amide. **B)** Gly-Pro alkene substitutions are potential  $n \rightarrow \pi^*$  acceptors from the Pro-Gly amide. **C)** Pro-Pro alkene substitutions are potential  $n \rightarrow \pi^*$  donors to the Pro-Gly amide. **D)** Pro-Pro alkene substitutions are potential  $n \rightarrow \pi^*$  acceptors from the Gly-Pro amide.

Only the torsion angles of the bonds that mimic the  $\Psi$ -bonds of Gly-Pro or Pro-Pro models were scanned because the  $\Phi$ -bonds of these models are conformationally constrained by the 5-membered rings. The  $\Phi$ -bonds of PG(-X)=P mimics are conformationally mobile, so they were restricted to the collagen-like peptide angle ( $72^\circ$ ).<sup>16</sup> The relative energies of all conformational

minima, maxima, and NBO<sup>37</sup> interactions are compared to our previous work on the conformational energy landscape of collagen PPII model amides GPP, PGP, and PPG.<sup>16</sup> The Bürgi–Dunitz parameters of PPII-like geometries are directly compared with the average conformations found in the high-resolution (1.3 Å) crystal structure of the collagen-like peptide (Gly–Pro–Pro)<sub>10</sub> (PDB ID: 1K6F).<sup>6</sup> Each model’s PPII-like minimum conformation was superimposed on PDB ID: 1K6F.<sup>6</sup>

### *Gly–Pro Alkene Isosteres*

The  $\Psi$  dihedral angle scans for G(–X)=PP donor models (Figure 3A) and PG(–X)=P acceptor models (Figure 3B) are overlaid with their respective GPP and PGP amide coordinate scans at the MP2/6-31+G(d) level of theory.<sup>16</sup> A complete list of geometric and Bürgi–Dunitz parameters for all minima and maxima calculated at the MP2/6-311+G(2d,p) level can be found in Supporting Information Table S1. The closest minimum to the PPII-like  $\Psi$  dihedral angle in each series was analyzed further to determine conformational compatibility with collagen, and the presence or absence of a stabilizing  $n \rightarrow \pi^*$  interaction.

For the G(–X)=PP donor series, all models have their global minima near the GPP *D/A1* global minimum at  $\Psi = +160^\circ$  (Figure 3A). These will be discussed in detail below. Both fluoro- and chloro-alkene donor models have local minima near  $\Psi = -20^\circ$  that are about 2 kcal/mol less stable than their respective global minima, as was found for the GPP amide *D/A1* (Table S1).<sup>16</sup> The G(–F)=PP local minimum at  $\Psi = -18^\circ$  has no discernible  $n \rightarrow \pi^*$  or hydrogen bonding interactions (Figure S1A). The G(–Cl)=PP local minimum at  $\Psi = -19^\circ$  is stabilized by an  $n \rightarrow si-\pi^*$  interaction (Figure S1B). A similar  $n \rightarrow si-\pi^*$  interaction is seen with the amide GPP *D/A1* at  $\Psi = -17^\circ$  (Table S1).<sup>16</sup> The only comparable local minimum for the proteo-alkene G(–H)=PP is found near  $\Psi = -$

60° where a stabilizing  $\sigma \rightarrow \pi^*$  interaction is seen (Figure S1C).

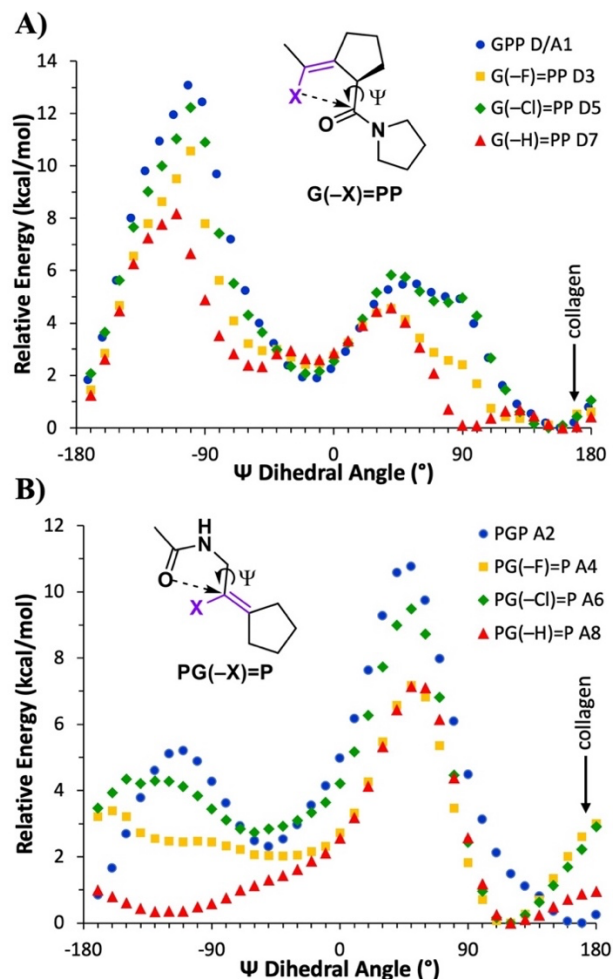


**Figure 3.** Potential energy scans of the  $\Psi$  dihedral angle in models of Gly-Pro amide substitutions where  $X = F, Cl, \text{ or } H$ . **A)**  $G(-X)=PP$   $n \rightarrow \pi^*$  donor, and **B)**  $PG(-X)=P$   $n \rightarrow \pi^*$  acceptor models overlaid with their respective PPII amide model energies as a function of  $\Psi$ .<sup>16</sup> The global minimum for each model was normalized to 0.0 kcal/mol. The average collagen  $\Psi$  dihedral angle from PDB ID: 1K6F in Table S3 is labeled.<sup>6</sup>

The local maxima between the global and local minima are all about 4 – 5 kcal/mol higher in energy than the global minima (Figure 3A). These maxima result from steric clashing between the

X group (or O in the case of the amide) and protons on the 5-membered ring. The global maxima for all models that are located around  $\Psi = +100^\circ$  are between 8 – 12 kcal/mol above the global minima (Figure 3A). These maxima are caused by steric clashing between the X group and the  $C_{i+1}=O$  oxygen.

For the PG(-X)=P acceptor series, all models have their global minima around  $\Psi = +120^\circ$ , which are within the same conformational energy well as the PPII-like PGP *A2* amide global minimum (Figure 3B). These are discussed in detail below. The PG(-F)=P and PG(-Cl)=P models have local minima around  $\Psi = -60^\circ$ , which are 2 – 3 kcal/mol higher in energy than their global minima (Table S1). An  $n \rightarrow \pi^*$  interaction is found at both halo-alkene local minima, but missing for PG(-H)=P (Figure S2).

The local maxima for both halo-alkenes around  $\Psi = -160^\circ$  are about 3 – 4 kcal/mol above the global minima (Figure 3B). These low-energy maxima are stabilized by reverse  $n \rightarrow \pi^*$  interactions (Figure S3A,B). The analogous local maximum for the PG(-H)=P model is missing this  $n \rightarrow \pi^*$  interaction (Figure S3C). The global maxima for all models located around  $\Psi = +50^\circ$  are about 7 – 9 kcal/mol higher in energy than the global minima (Figure 3B). These maxima correspond to eclipsing interactions between the X atom and one Gly  $H_\alpha$ , as well as the  $C_i=O$  oxygen and the other Gly  $H_\alpha$ .

#### *Gly-Pro Fluoro-alkene*

The G(-F)=PP *D3* donor model is the most geometrically similar mimic to GPP *D1* (Table 1). Unrestrained optimization of *D3* (global minimum) shows  $\Psi = +162^\circ$ , which is nearly identical to the GPP *D1* angle  $\Psi = +160^\circ$ , and superimposes very well with PDB ID: 1K6F (Figure 4A).<sup>6</sup> This suggests the G(-F)=PP isostere is a reasonably good mimic of the PPII conformation. This fluoro-

alkene **D3** global minimum has the Bürgi-Dunitz angle  $\tau_{BD} = 95^\circ$ , which is favorable for  $n \rightarrow \pi^*$  donation, although the distance  $\delta_{BD} = 3.3 \text{ \AA}$  is slightly above the  $3.17 \text{ \AA}$  sum of van der Waals radii (Table 1). Indeed, the NBO E2 energy of  $<0.1 \text{ kcal/mol}$  and NBO images (Figure 4B) suggest the lack of a significant  $n \rightarrow \pi^*$  interaction. Nevertheless, the  $n \rightarrow \pi^*$  interaction does not appear to be necessary to stabilize the PPII-like conformation of the G(-F)=PP model. Other non-bonding interactions beyond  $n \rightarrow \pi^*$  may play a greater role than expected to make the PPII-like conformation the global minimum.

**Table 1.** Key geometric parameters of average collagen structure, and the PPII-like global minima of the Gly-Pro amide and alkene models.

Model	$\Psi$ ( $^\circ$ )	$\pi^*$ face	$\delta_{BD}$ ( $\text{\AA}$ )	$\tau_{BD}$ ( $^\circ$ )	$\Theta_{BD}$ ( $^\circ$ )	NBO E2	rmsd ( $\text{\AA}$ ) 1K6F <sup>c</sup>
1K6F GPP <sup>a</sup>	+165		2.9	90			
1K6F PGP <sup>a</sup>	+176		3.1	90			
GPP <i>D/A1</i> <sup>b</sup>	+160	<i>re</i>	3.1	93	2.9	0.41	
PGP <i>A2</i> <sup>b</sup>	+167	-	3.2	89	0.2	0.19	
G(-F)=PP <b>D3</b>	+162	-	3.3	95	-	< 0.1	0.14
PG(-F)=P <b>A4</b>	+117	-	3.3	124	-	< 0.1	0.77
G(-Cl)=PP <b>D5</b>	+155	<i>re</i>	3.3	99	2.9	0.39	0.19
PG(-Cl)=P <b>A6</b>	+118	-	3.2	122	-	< 0.1	0.78
G(-H)=PP <b>D7</b>	+163	-	3.4	97	-	< 0.1	0.21
PG(-H)=P <b>A8</b>	+120	-	3.3	122	-	< 0.1	0.78

<sup>a</sup> Average  $\Psi$  angle,  $\delta_{BD}$  and  $\tau_{BD}$  from collagen crystal structure (PDB ID: 1K6F).<sup>6</sup> <sup>b</sup> Data for PPG

**D9** and GPP *D/A1* from reference <sup>16</sup>. <sup>c</sup> Superposition rmsd of model minima with PDB ID:

1K6F.<sup>6</sup>

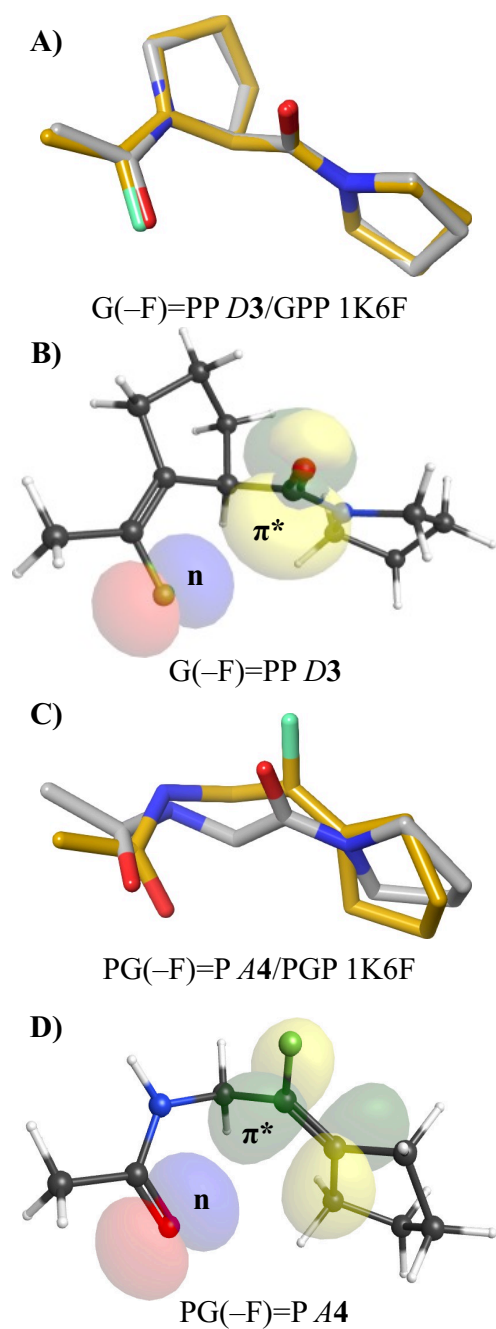


**Figure 4.** Gly-Pro fluoro-alkene models calculated at the MP2/6-311+G(2d,p) level. **A)** G(-F)=PP *D3* (gold) superimposed on PDB ID: 1K6F (grey). **B)** G(-F)=PP *D3* NBOs show no overlap between fluorine n orbital (blue/red) and C=O  $\pi^*$  orbital (green/yellow). **C)** PG(-F)=P *A4* (gold) superimposed on PDB ID: 1K6F (grey). **D)** PG(-F)=P *A4* NBOs show no overlap between oxygen

n orbital (blue/red) and C=C  $\pi^*$  orbital (green/yellow).

The PG(-F)=P **A4** acceptor model global minimum is notably shifted from the PGP **A2** PPII-like geometry (Figure 3B). Unrestrained optimization of **A4** gives  $\Psi = +117^\circ$ , which deviates significantly from the amide PGP **A2** at  $\Psi = +167^\circ$  (Table 1). This conformation does not superimpose well with the PGP 1K6F fragment,<sup>6</sup> which suggests that **A2** is not a good fit for the PPII conformation (Figure 4C). However, since the global minimum is only about 2 kcal/mol lower in energy than the PPII conformation, and within the same energy well, the PPII conformation still appears to be thermally accessible. The global minimum of **A4** has  $\delta_{BD} = 3.3 \text{ \AA}$  and  $\tau_{BD} = 124^\circ$ , and an NBO E2 energy  $< 0.1 \text{ kcal/mol}$ , all of which point to the absence of an  $n \rightarrow \pi^*$  interaction (Table 1, Figure 4D). Since the donor conformation is PPII-like, and the acceptor deviates, some compromise is expected to occur in the collagen triple helix.

#### *Gly-Pro Chloro-alkene*

The  $\Psi$ -conformational energy profile of donor model G(-Cl)=PP **D5** closely resembles that of the amide GPP **D/A1** (Figure 3A). The unrestrained optimized geometry of **D5** at its global minimum has  $\Psi = +155^\circ$  (Table 1). The superposition of **D5** with 1K6F shows very favorable alignment,<sup>6</sup> suggesting that the chloro-alkene could mimic the PPII conformation well (Figure 5A). **D5** has Bürgi-Dunitz parameters  $\delta_{BD} = 3.3 \text{ \AA}$  and  $\tau_{BD} = 99^\circ$ , which are within the geometric limits for a sizable  $n \rightarrow \pi^*$  interaction (Table 1). The presence of  $n \rightarrow \pi^*$  donation is supported by pyramidalization of  $C_{i+1}=O$  carbon with  $\theta_{BD} = 2.9^\circ$  (Table 1). The NBO E2 energy of 0.39 kcal/mol (Table 1) supports the presence of an  $n \rightarrow \pi^*$  interaction, depicted with NBOs in Figure 5B.

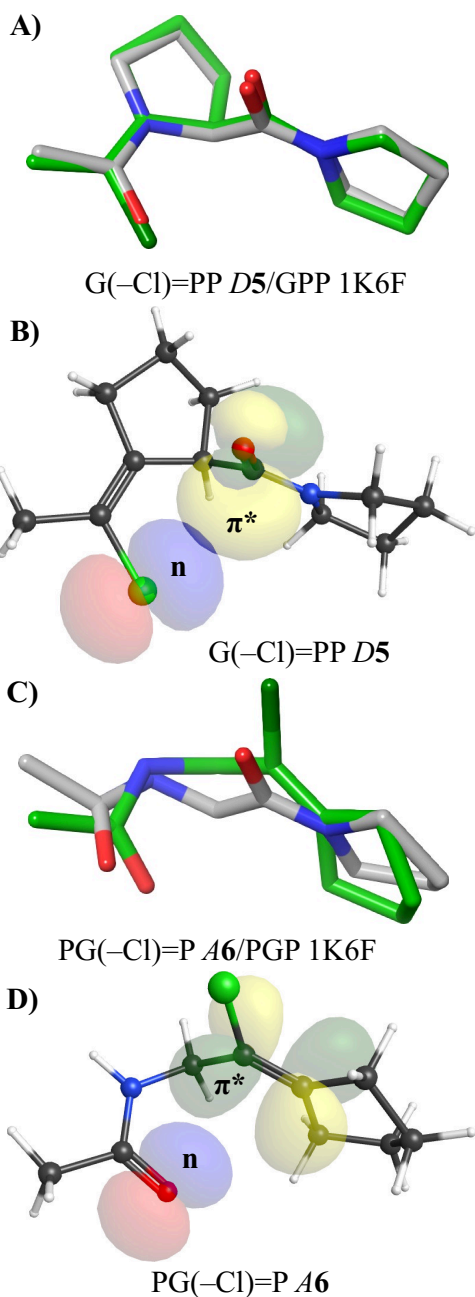


**Figure 5.** Gly-Pro chloro-alkene models calculated at the MP2/6-311+G(2d,p) level. **A)** G(-Cl)=PP *D5* (green) superimposed on PDB ID: 1K6F (grey). **B)** G(-Cl)=PP *D5* NBOs show overlap between chlorine n orbital (blue/red) and C=O  $\pi^*$  orbital (green/yellow). **C)** PG(-Cl)=P *A6* (green) superimposed on PDB ID: 1K6F (grey). **D)** PG(-Cl)=P *A6* NBOs show no overlap between oxygen n orbital (blue/red) and C=C  $\pi^*$  orbital (green/yellow).



The corresponding acceptor model, PG(-Cl)=P *A6*, does not have favorable PPII geometry when overlaid with the PGP portion of 1K6F (Figure 5C).<sup>6</sup> The global minimum of *A6* exhibits  $\Psi = +118^\circ$ , which diverges considerably from the PPII global minimum conformation of PGP *A2* ( $\Psi = +167^\circ$ , Table 1). Again, since the potential energy surface around the global minimum is very isotropic, and the *A6* conformation is only about 2 kcal/mol higher in energy than that of the PPII conformation, the PPII conformation is still accessible to PG(-Cl)=P. Interestingly, *A6* has  $\delta_{BD} = 3.2 \text{ \AA}$ , which is within the expected distance for an  $n \rightarrow \pi^*$  interaction with a chlorine, and the Bürgi-Dunitz angle of  $\tau_{BD} = 122^\circ$  is only  $13^\circ$  higher than the optimal  $109^\circ$ , yet it appears to lack an  $n \rightarrow \pi^*$  interaction (Table 1). The NBO E2 energy is less than 0.1 kcal/mol (Table 1) suggesting no significant orbital interactions, as can be appreciated in the NBO images (Figure 5D). Besides the lack of favorable conformation, the Gly-Pro chloro-alkene mimic is expected to disrupt triple helix formation due to the long C-Cl bond, and the size of Cl.

#### *Gly-Pro Proteo-alkene*

The torsional energy profile of donor model G(-H)=PP *D7* has two low-energy minima at  $\Psi = +160^\circ$  and  $\Psi = +100^\circ$  (Figure 3A). Full optimizations starting from each geometry show the true global minimum lies at  $\Psi = +96^\circ$ , while the PPII-like  $\Psi = +163^\circ$  is a local minimum that is only 0.20 kcal/mol higher in energy, and with an estimated barrier between them of  $\Delta E = 0.82 \text{ kcal/mol}$  (Table S1). The PPII-like minimum of G(-H)=PP *D7* can mimic the PPII conformation well, as evidenced by its superposition on GPP from 1K6F (Figure 6A).<sup>6</sup> However, the broad, shallow conformational energy profile around the global minimum helps to explain the known destabilization of the collagen-like triple helix we reported with a Gly-Pro proteo-alkene.<sup>13</sup> The alkene *D7* minimum at  $\Psi = +163^\circ$  has the Bürgi-Dunitz angle  $\tau_{BD} = 97^\circ$ , which is favorable for

$n \rightarrow \pi^*$  donation, although the distance  $\delta_{BD} = 3.4 \text{ \AA}$  is highly unfavorable for a C–H---C=O interaction (Table 1). The NBO image also shows no C–H  $\sigma \rightarrow \pi^*$  overlap (Figure 6B), which is verified by the lack of NBO E2 energy for the interaction (Table 1).

The energy profile of acceptor model PG(–H)=P **A8** has minima at  $\Psi = +120^\circ$  and  $\Psi = -120^\circ$  (Figure 3B). Unrestrained optimization of both minima puts the global minimum at  $\Psi = +120^\circ$  (Table 1) and a broad, shallow local minimum at  $\Psi = -119^\circ$  only 0.2 kcal/mol higher in energy, with a low estimated barrier of  $\Delta E = 1.2$  kcal/mol between them (Table S1). The global minimum of **A8** does not superimpose well with the PPII conformation of 1K6F,<sup>6</sup> again helping to explain the destabilization of collagen-like peptides by a Gly–Pro proteo-alkene mimic (Figure 6C).<sup>13</sup> The high flexibility of this model is not stabilized by an  $n \rightarrow \pi^*$  interaction based on its Bürgi-Dunitz parameters, NBO E2 energy, and NBO images (Table 1, Figure 6D).

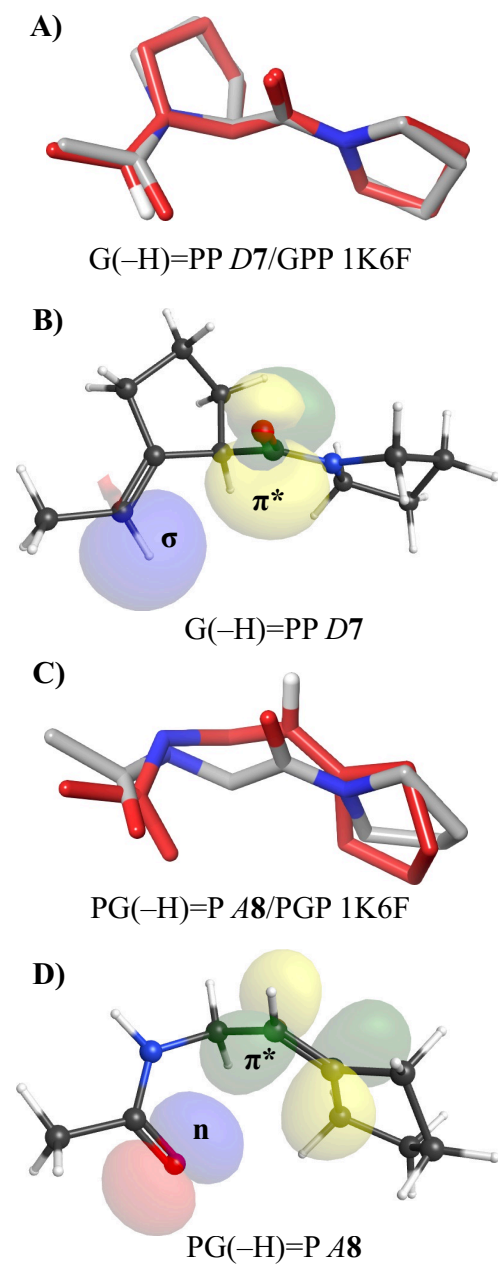


**Figure 6.** Gly-Pro proteo-alkene models calculated at the MP2/6-311+G(2d,p) level. **A)** G(-H)=PP *D7* (red) superimposed on PDB ID: 1K6F (grey). **B)** G(-H)=PP *D7* NBOs show no overlap between the C-H  $\sigma$  orbital (blue/red) and C=O  $\pi^*$  orbital (green/yellow). **C)** PG(-H)=P *A8* (red) superimposed on PDB ID: 1K6F (grey). **D)** PG(-H)=P *A8* NBOs show no overlap between oxygen n orbital (blue/red) and C=C  $\pi^*$  orbital (green/yellow).

### *Pro-Pro Alkene Isosteres*

Although fluorine and chlorine atoms have been known to establish hydrogen bonding interactions,<sup>42, 43</sup> substitution of the Pro-Pro amide may prove problematic due to weaker C–X···H–N compared to C=O···H–N interstrand hydrogen bonds that strengthens the interactions between the three strands of the collagen triple helix (Figure S4).<sup>33</sup> We include the following Pro-Pro model conformational analyses to see how well the fluoro- or chloro-alkenes might mimic the PPII conformation, and to help explain the failure of the Pro-Pro proteo-alkene isostere to stabilize the collagen-like triple helix beyond the missing interstrand hydrogen bond.<sup>14</sup> The  $\Psi$  dihedral angle coordinate scans for P(–X)=PG donor models (Figure 7A) and GP(–X)=P acceptor models (Figure 7B) are overlaid with their respective PPG *D9* and GPP *D/A1* amide coordinate scans at the MP2/6-31+G(d) level of theory.<sup>16</sup> A complete list of geometric and Bürgi-Dunitz parameters for all minima and maxima calculated at the MP2/6-311+G(2d,p) level can be found in Supporting Information Table S2.

The PPII-like amide minimum of PPG *D9* is not the global minimum, which indicates that other long-range forces, such as Pro C=O···H–N Gly interstrand hydrogen bonds, contribute to the stabilization of the collagen triple helix, even for native amides.<sup>16</sup> The PPII-like minima for all models in the P(–X)=PG donor series are also local, not global, minima that are approximately 1 – 2 kcal/mol higher in energy than their respective global minima (Figure 7A). These PPII-like minima are discussed in detail below.

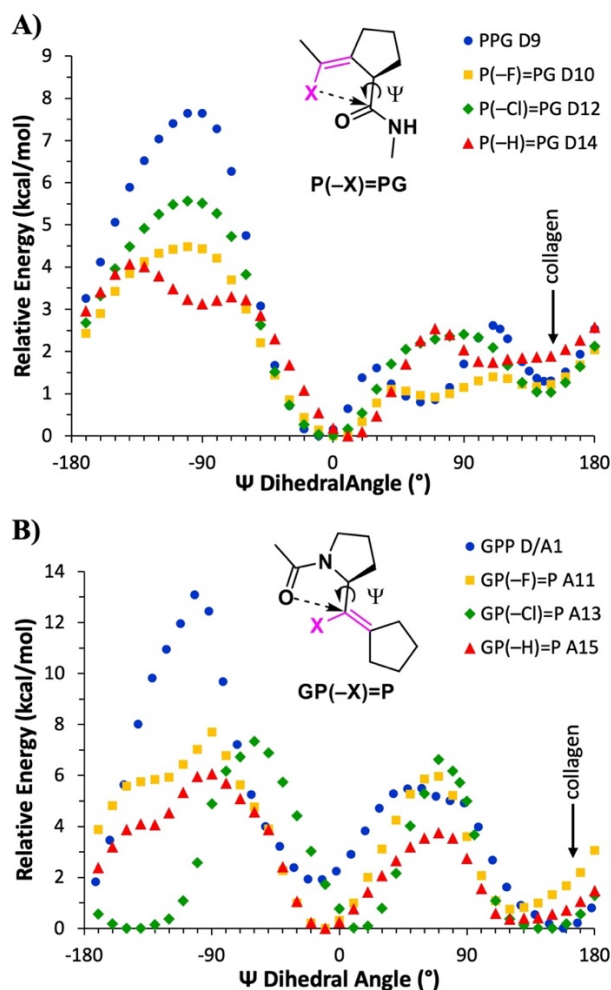


**Figure 7.** Potential energy scans of the  $\Psi$  dihedral angle in models of Pro-Pro amide substitutions where  $X = F, Cl,$  or  $H$ . **A)**  $P(-X)=PG$   $n \rightarrow \pi^*$  donor, and **B)**  $GP(-X)=P$   $n \rightarrow \pi^*$  acceptor models overlaid with their respective PPII-like amide model energies as a function of  $\Psi$ .<sup>16</sup> The global minimum for each model was normalized to 0.0 kcal/mol. The average collagen  $\Psi$  dihedral angle from PDB ID: 1K6F in Table S3 is labeled.<sup>6</sup>

All three alkene models were found to have their global minima between  $\Psi = -15^\circ$  and  $\Psi = +15^\circ$  (Figure 7A). This geometry includes an alkene  $C_i=C_{i+1} \pi \cdots H-N_{i+2}$  intramolecular hydrogen bond (Table S2, Figure S5). Intramolecular alkene  $\pi \cdots H-N$  hydrogen bonding has been found

experimentally.<sup>44</sup> This minimum is also reported for the amide PPG *D9* as an  $N_{i+1}\cdots H-N_{i+2}$  hydrogen bond (Table S2, Figure S5D).<sup>16</sup>

Of the alkene models, only P(-F)=PG *D10* has a local minimum at  $\Psi = +64^\circ$ , which is about 1 kcal/mol higher in energy than the global minimum (Figure 7A). This conformation features an inverse  $\gamma$ -turn with an intramolecular 7-membered ring closed by a  $C_i-F\cdots H-N_{i+1}$  hydrogen bond (Figure S6A). A similar  $C_i=O\cdots H-N_{i+1}$  hydrogen bond is found for PPG *D9* at  $\Psi = +62^\circ$  (Figure S6B).<sup>16</sup> Such an interaction is unique to the fluoro-alkene mimic; of course, analogous hydrogen bonds are not seen in either chloro- or proteo-alkene models.

For these Pro-Pro donor alkene models, the global maxima at  $\Psi = -100^\circ$ , resulting from an eclipsing interaction between the X atom (or oxygen for the amide) and a proton on the 5-membered ring, are 4 to 6 kcal/mol higher in energy than the global minima. The alkene hydrogen of P(-H)=PG *D14* is too small to be sterically hindered in this way, and instead has an eclipsing interaction between the  $N_{i+1}-H$  and the 5-membered ring around  $\Psi = -140^\circ$  (Figure 7A).

The GP(-X)=P acceptor model conformation scans are comparable to the native amide GPP *D/A1* scan, which has an energy difference of 1.7 kcal/mol between its PPII-like global minimum at  $\Psi = +160^\circ$  and a local minimum around  $\Psi = -20^\circ$ , with a large 5.1 kcal/mol barrier between them (Table S2).<sup>16</sup> The PPII-like local minima for all GP(-X)=P acceptor models are between 0.5 – 1 kcal/mol less stable than their respective global minimum (Figure 7B).

The scans of the GP(-F)=P *A11* and GP(-H)=P *A15* acceptor models are conformationally similar (Figure 7B). The global minima of both models are sterically favored conformations around  $\Psi = -10^\circ$  with no H-bond or  $n\rightarrow\pi^*$  interactions (Figures S7A, S7B). In a collagen-like peptide, the GP(-F)=P alkene mimic is expected to have similar challenges as the previously synthesized GP(-

H)=P mimic.<sup>14</sup> The GP(-Cl)=P **A13** global minimum is located around  $\Psi = +10^\circ$  and is stabilized by a weak  $n \rightarrow \pi^*$  interaction (Figure S7C). For all GP(-X)=P acceptor models, the maxima around  $\Psi = +70^\circ$  are due to eclipsing interactions between the X atom (or oxygen for amide) and the 5-membered ring (Figure 7B).

#### *Pro-Pro Fluoro-alkene*

Unrestrained optimization of the most PPII-like minimum of donor model P(-F)=GP **D10** gives  $\Psi = +142^\circ$ , which is 1.4 kcal/mol above the global minimum at  $\Psi = +1^\circ$  (Table 2). This torsion angle is relatively close to that of the PPG **D9** PPII-like minimum at  $\Psi = +150^\circ$ , which is similarly 1.0 kcal/mol above the global minimum (Table 2). The **D10** conformation superimposes reasonably well with the PPG segment of 1K6F,<sup>6</sup> which suggests that a Pro-Pro fluoro-alkene mimic could be geometrically compatible with the triple helix (Figure 8A). Additionally, **D10** has ideal Bürgi-Dunitz parameters with  $\delta_{BD} = 3.1 \text{ \AA}$  and  $\tau_{BD} = 104^\circ$  (Table 2). Our calculations show pyramidalization of the  $C_{i+1}=O$  carbon by  $\theta_{BD} = 2.2^\circ$ , and an NBO E2 energy of 0.16 kcal/mol. The weak  $n \rightarrow \pi^*$  interaction can be visualized in Figure 8B.

The fluoro-alkene acceptor model, GP(-F)=P **A11**, has an unfavorable energy landscape for a PPII mimic (Figure 7B). Unrestrained optimization of its most PPII-like minimum gives  $\Psi = +123^\circ$  at 1.0 kcal/mol above the global minimum (Table 2). The significant difference compared to the collagen GPP **D/A1** geometry at  $\Psi = +160^\circ$ , and its inadequate superposition with 1K6F, may preclude it as a PPII mimic (Figure 8C). However, the **A11** conformation is within the same energy well as the PPII-like conformation at  $\Psi = +160^\circ$  (Figure 7B). Interestingly, **A11** has good Bürgi-Dunitz parameters with  $\delta_{BD} = 3.2 \text{ \AA}$  and  $\tau_{BD} = 118^\circ$  (Table 2); however, NBO images and E2 energies agree on the absence of strong orbital overlap (Figure 8D, Table 2). Whether a Pro-Pro

fluoro-alkene mimic would provide a sufficient interstrand H-bond acceptor remains an open question.

**Table 2.** Key geometric parameters of the collagen structure, and the PPII-like minima of Pro–Pro amide and alkene models.

Model	$\Psi$ (°)	$\Delta E^c$	$\pi^*$ face	$\delta_{BD}$ (Å)	$\tau_{BD}$ (°)	$\theta_{BD}$ (°)	NBO E2	rmsd (Å) 1K6F <sup>d</sup>
1K6F PPG <sup>a</sup>	+152			3.1	81			
1K6F GPP <sup>a</sup>	+165			2.9	90			
PPG <b>D9</b> <sup>b</sup>	+150	1.0	<i>re</i>	3.0	98	3.0	0.46	
GPP <b>D/A1</b> <sup>b</sup>	+160	0.0	<i>re</i>	3.1	93	2.9	0.41	
P(-F)=PG <b>D10</b>	+142	1.4	<i>re</i>	3.1	104	2.2	0.16	0.32
GP(-F)=P <b>A11</b>	+123	1.0	-	3.2	118	-	<0.1	0.54
P(-Cl)=PG <b>D12</b>	+147	1.2	<i>re</i>	3.3	104	2.6	0.45	0.35
GP(-Cl)=P <b>A13</b>	+145	0.5	<i>re</i>	3.1	99	1.6	0.20	0.25
P(-H)=PG <b>D14</b>	+101	1.8	-	3.0	130	-	<0.1	0.56
GP(-H)=P <b>A15</b>	+120	0.6	-	3.3	123	-	<0.1	0.53

<sup>a</sup> Average  $\Psi$  angle,  $\delta_{BD}$  and  $\tau_{BD}$  from collagen crystal structure (PDB ID: 1K6F).<sup>6</sup> <sup>b</sup> Data for PPG

**D9** and GPP **D/A1** from reference <sup>16</sup>. <sup>c</sup> Energy relative to the respective global minimum

(kcal/mol). <sup>d</sup> Superposition rmsd of model minima with PDB ID: 1K6F.<sup>6</sup>



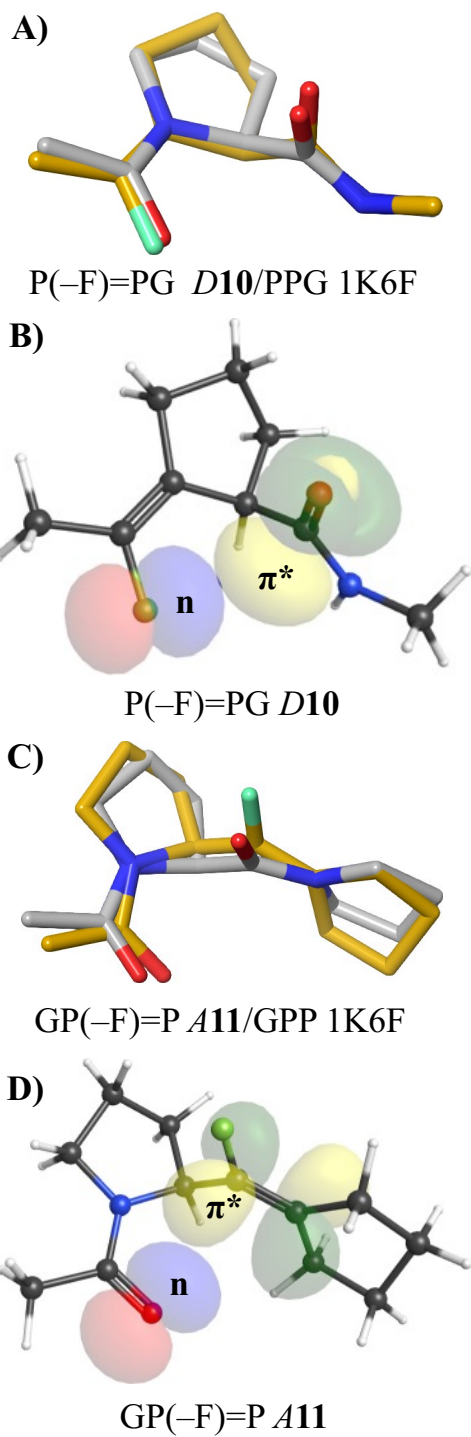


**Figure 8.** Pro-Pro fluoro-alkene models calculated at the MP2/6-311+G(2d,p) level. **A)** P(-F)=PG *D10* (gold) superimposed on PDB ID: 1K6F (grey). **B)** P(-F)=PG *D10* NBOs show limited overlap between fluorine n orbital (blue/red) and C=O  $\pi^*$  orbital (green/yellow). **C)** GP(-F)=P *A11* (gold)

superimposed on PDB ID: 1K6F (grey). **D**) GP(-F)=P **A11** NBOs show no overlap between oxygen n orbital (blue/red) and C=C  $\pi^*$  orbital (green/yellow).

### *Pro-Pro Chloro-alkene*

Unrestrained optimization of the PPII-like minimum of the chloro donor model P(-Cl)=PG **D12** converges to  $\Psi = +147^\circ$  (Table 2). This structure is geometrically very similar to amide model PPG **D9** with  $\Psi = +150^\circ$ , and it shows reasonably good superposition on the PPII segment of 1K6F (Figure 9A).<sup>6</sup> **D12** also has good Bürgi-Dunitz parameters with  $\delta_{\text{BD}} = 3.3 \text{ \AA}$  and  $\tau_{\text{BD}} = 104^\circ$  (Table 2). The NBO E2 energy (0.45 kcal/mol) confirms an  $n \rightarrow \pi^*$  interaction, which can be visualized in Figure 9B. The presence of  $n \rightarrow \pi^*$  donation is further supported by the pyramidalization of the  $\text{C}_{i+1}=\text{O}$  carbon,  $\theta_{\text{BD}} = 2.6^\circ$  (Table 2).

The coordinate scan of the GP(-Cl)=P **A13** acceptor model has two minima at  $\Psi = +140^\circ$  and  $\Psi = -140^\circ$  (Figure 7B). Unrestrained optimization of both structures converged to the same point at  $\Psi = +145^\circ$ , which is not far from the PPII-like GPP **D/A1** conformation at  $\Psi = +160^\circ$  (Table 2). Model **A13** also shows good superposition with the PPII in 1K6F, so this mimic is expected to mimic the PPII conformation well (Figure 9C).<sup>6</sup> The fully optimized model has  $\delta_{\text{BD}} = 3.1 \text{ \AA}$  and  $\tau_{\text{BD}} = 99^\circ$ , which are ideal parameters for  $n \rightarrow \pi^*$  donation to occur (Table 2). Remarkably, an NBO E2 energy of 0.20 kcal/mol and carbon pyramidalization  $\theta_{\text{BD}} = 1.65^\circ$  suggest this chloroalkene can also act as an  $n \rightarrow \pi^*$  acceptor (Table 2). This is further supported by the NBO image (Figure 9D). What is perhaps most interesting about this  $n \rightarrow \pi^*$  interaction is that it occurs despite repulsion between the oxygen lone pair and the  $\pi$ -bonding orbital (Figure S7B).

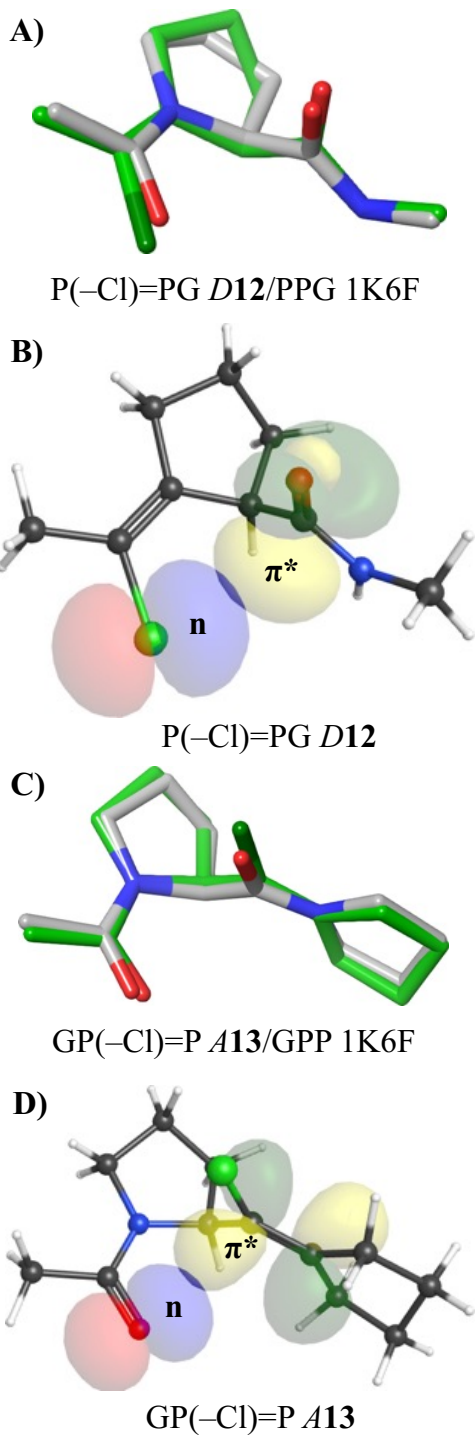


**Figure 9.** Pro-Pro chloro-alkene models calculated at the MP2/6-311+G(2d,p) level. **A)** P(-Cl)=PG *D12* (green) superimposed on PDB ID: 1K6F (grey). **B)** P(-Cl)=PG *D12* NBOs show strong overlap between chlorine n orbital (blue/red) and C=O  $\pi^*$  orbital (green/yellow). **C)** GP(-

Cl)=P **A13** (green) superimposed on PDB ID: 1K6F (grey). **D**) GP(-Cl)=P **A13** NBOs show an  $n \rightarrow \pi^*$  interaction between oxygen n orbital (blue/red) and C=C  $\pi^*$  orbital (green/yellow).

Although the Pro-Pro chloro-alkene models mimic the PPII conformation very well, we expect that the chloroalkene would destabilize collagen-like peptides because of the long C-Cl bond, the size of the Cl, and the need for a triple-helix interstrand hydrogen-bond acceptor atom at this position. However, this chloroalkene might serve to stabilize a PPII helix that is not part of a triple helix.

#### *Pro-Pro Proteo-alkene*

Unrestrained optimization of donor model P(-H)=PG **D14** results in a broad minimum at  $\Psi = +101^\circ$ , which is 1.8 kcal/mol above its global minimum at  $\Psi = +12^\circ$  (Table 2). This differs considerably from the PPII-like minimum of PPG **D9** at  $\Psi = +150^\circ$  that is 1.0 kcal/mol above the global minimum (Table 2). Model **D14** does not overlap well with the PPII segment in 1K6F (Figure 10A).<sup>6</sup> The geometric parameters,  $\delta_{BD} = 3.0 \text{ \AA}$  and  $\tau_{BD} = 130^\circ$ , are outside the ideal Bürgi-Dunitz threshold for hydrogen (Table 2). Both NBO E2 energy and NBO images indicate no significant overlap of the C-H  $\sigma$  and C=O  $\pi^*$  orbitals (Figure 10B).

Acceptor model GP(-H)=P **A15** also exhibits an energetic landscape unfavorable to PPII stabilization (Figure 7B). The unrestrained optimized structure of its global minimum gives  $\Psi = +120^\circ$  compared to the amide GPP **D/A1** with  $\Psi = +160^\circ$  (Table 2). Model **A15** also shows very poor superposition on GPP from 1K6F (Figure 10C).<sup>6</sup> The Bürgi-Dunitz parameters of  $\delta_{BD} = 3.3 \text{ \AA}$  and  $\tau_{BD} = 123^\circ$  are inadequate for a strong  $n \rightarrow \pi^*$  interaction (Table 2). The NBO E2 energy of less than 0.1 kcal/mol and the NBO images show no significant  $n \rightarrow \pi^*$  overlap (Figure 10D).

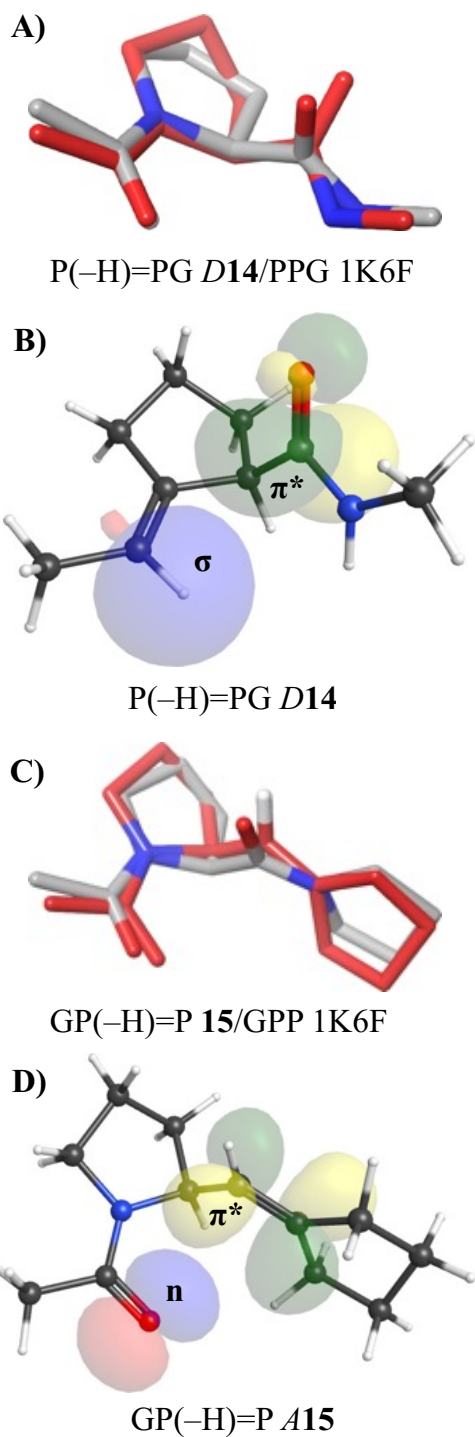


**Figure 10.** Pro-Pro proteo-alkene models calculated at the MP2/6-311+G(2d,p) level. **A)** P(-H)=PG *D14* (red) superimposed on PDB ID: 1K6F (grey). **B)** P(-H)=PG *D14* NBOs show no interaction between the C-H  $\sigma$  orbital (blue/red) and C=O  $\pi^*$  orbital (green/yellow). **C)** GP(-H)=P

**A15** (red) superimposed on PDB ID: 1K6F (grey). **D**) GP(-H)=P **A15** NBOs show no interaction between oxygen n orbital (blue/red) and C=C  $\pi^*$  orbital (green/yellow).

The shallow conformational energy surfaces for both donor and acceptor Pro-Pro proteo-alkene models, the large differences in  $\Psi$  torsion angles from the PPII-helix, poor overlap with a collagen-like peptide, and the lack of stabilizing non-covalent interactions, help to explain the experimental destabilizing effect of our Pro-Pro proteo-alkene mimic in a collagen-like peptide.<sup>14</sup>

## Conclusions

Halo-alkene isosteres are interesting as potential collagen mimics, since their global minima or low-lying local minima are near the PPII-like conformation in our models. Both Gly-Pro fluoro- and chloro-alkene  $n \rightarrow \pi^*$  donor models are stable in the conformation that is most similar to the PPII conformation. An  $n \rightarrow \pi^*$  interaction is found in the Gly-Pro donor model G(-Cl)=PP **D5**, as well as Pro-Pro donor models P(-F)=PG **D10**, P(-Cl)=PG **D11**, and acceptor model GP(-Cl)=P **A13**. The halo-alkenes serve well as  $n \rightarrow \pi^*$  donors, but the conformations are altered in the models in which the halo-alkenes serve as  $n \rightarrow \pi^*$  acceptors, shifting the lowest energy conformation to about  $\Psi = +120^\circ$ , instead of the PPII-like  $\Psi = +145^\circ$  to  $+160^\circ$ . The Pro-Pro chloro-alkene mimic is an exception because it captures the native amide conformations in both the donor and acceptor models. In situations where acceptor minima are different from PPII-like minima, the donor interactions may provide counterbalance, suggesting they could serve as conformationally restricted isosteres for collagen. The lack of  $n \rightarrow \pi^*$  interactions in some of the PPII-like minima of the models that actually mimic PPII well suggests that other non-bonding interactions may be greater forces than expected.

All  $n \rightarrow \pi^*$  interactions are missing entirely from models of our previously reported Gly-Pro and

Pro–Pro proteo-alkene mimics in collagen-like peptides.<sup>13, 14</sup> In addition, interactions with other strands within a triple helix are not captured in our models, which may provide additional stabilizing or destabilizing forces. Further computational and/or experimental studies are necessary to fully answer these questions.

If the polarity and size of the amide bond dominates triple-helix folding, then we expect the fluoro-alkene to be the better mimic. However, if an  $n \rightarrow \pi^*$  interaction is critical for folding, we expect the chloro-alkene to be a better mimic. Further, we predict that substitution at the Gly–Pro position will provide more stability than substitution at the Pro–Pro position, because chlorine and fluorine are unlikely to be good interstrand hydrogen-bond acceptors in the collagen triple helix. The Gly–Pro haloalkene mimics are currently under experimental investigation.

## AUTHOR INFORMATION

Corresponding Author

\*(F.A.E.) E-mail: [fetzkorn@vt.edu](mailto:fetzkorn@vt.edu).

## ORCID

Felicia A. Etzkorn: [0000-0001-5850-3661](https://orcid.org/0000-0001-5850-3661)

Diego Troya: [0000-0003-4971-4998](https://orcid.org/0000-0003-4971-4998)

## ASSOCIATED CONTENT

### **Supporting Information**

The following files are available free of charge. Geometric parameters of models at all minima

and maxima optimized at MP2/6-311+G(2d,p) including  $\Psi$  and  $\Phi$  angles,  $\Delta E$ ,  $\pi^*$ -bond face of  $n \rightarrow \pi^*$  interactions,  $\delta_{BD}/d_{HB}$ ,  $\tau_{BD}/\angle_{HB}$ ,  $\theta_{BD}$ , and NBO E2 energy (Tables S1 – S2); average  $\Psi$  and  $\Phi$  dihedral angles of PDB ID: 1K6F (Table S3); average  $\delta_{BD}$  and  $\tau_{BD}$  angles of PDB ID: 1K6F (Table S4); non-covalent interactions in non-PPII-like geometries (Figures S1 – S7). (PDF)

Gly–Pro Amide Substitution.xlsx: Energies,  $\Psi$  angles for scans, and energies, distances, and angles for all optimized models ([XLSX](#))

Pro–Pro Amide Substitution.xlsx: Energies,  $\Psi$  angles for scans, and energies, distances, and angles for all optimized models ([XLSX](#))

Arcoria-Supplemental-Coordinates.zip “Output Coordinates,” cartesian coordinates of model geometries at all energy minima and maxima described in Tables S1 and S2. “Representative Input Files,” contains a sample input for each type of calculation performed: the coordinate scan, optimization and NBO of the collagen-like minimum, and the TS single point calculation of GP(–F)=P *A11* (Table S2). (ZIP)

## ACKNOWLEDGMENT

The authors acknowledge Advanced Research Computing at Virginia Tech for providing computational resources and technical support that have contributed to the results reported within this paper, and the NSF for grant CHE-0749061. They thank Anne M. Brown (University Libraries, Virginia Tech) and Erin T. Collin (Virginia Tech) for the use of, and help with, Schrödinger software. No competing financial interests have been declared.

## ABBREVIATIONS



$\delta_{\text{BD}}$  = Bürgi–Dunitz distance;  $\tau_{\text{BD}} = \angle \text{O}_i\text{---C}_{i+1}=\text{O}$ , Bürgi–Dunitz angle;  $\Theta_{\text{BD}}$  = Bürgi–Dunitz pyramidalization angle;  $d_{\text{HB}}$  = hydrogen-bond distance;  $\angle_{\text{HB}}$  = hydrogen-bond angle; PPII = polyproline type II; PPG = Pro–Pro–Gly; PGP = Pro–Gly–Pro; GPP = Gly–Pro–Pro;  $\Phi$  = dihedral angle/bond  $\text{C}'_i\text{---N}_{i+1}\text{---C}\alpha_{i+1}\text{---C}'_{i+1}$ ;  $\Psi$  = dihedral angle/bond  $\text{N}_i\text{---C}\alpha_i\text{---C}'_i\text{---N}_{i+2}$ ; MP2 = Møller–Plesset-2; NBOs = natural bond orbitals

## References

1. Shoulders, M. D.; Raines, R. T., Collagen Structure and Stability. *Annu. Rev. Biochem.* **2009**, *78*, 929-958.
2. Rich, A.; Crick, F. H. C., The Molecular Structure of Collagen. *J. Mol. Biol.* **1961**, *3*, 483-506.
3. Brodsky, B.; Shah, N. K., The Triple-Helix Motif in Proteins. *FASEB J.* **1995**, *9*, 1537-1546.
4. Adzhubei, A. A.; Sternberg, M. J. E.; Makarov, A. A., Polyproline-II Helix in Proteins: Structure and Function. *J. Mol. Biol.* **2013**, *425*, 2100-2132.
5. Ramshaw, J. A.; Shah, N. K.; Brodsky, B., Gly-X-Y Tripeptide Frequencies in Collagen A Context for Host-Guest Triple-Helical Peptides. *J. Struct. Biol.* **1998**, *122*, 86-91.
6. Berisio, R.; Vitagliano, L.; Mazzarella, L.; Zagari, A., Crystal Structure of the Collagen Triple Helix Model [(Pro–Pro–Gly)<sub>(10)</sub>]<sub>(3)</sub>. *Protein Sci.* **2002**, *11*, 262-70.
7. DeRider, M. L.; Wilkens, S. J.; Waddell, M. J.; Bretscher, L. E.; Weinhold, F.; Raines, R. T.; Markley, J. L., Collagen Stability: Insights from NMR Spectroscopic and Hybrid Density Functional Computational Investigations of the Effect of Electronegative Substituents on Prolyl Ring Conformations. *J. Am. Chem. Soc.* **2002**, *124*, 2497-2505.
8. Brandts, J. F.; Halvorson, H. R.; Brennan, M., Consideration of the Possibility That the Slow Step in Protein Denaturation Reactions is Due to Cis-Trans Isomerism of Proline Residues. *Biochemistry* **1975**, *14*, 4953-63.
9. Bachinger, H., P.; Engel, J.; Bruckner, P.; Timpl, R., The Role of Cis-Trans Isomerization of Peptide Bonds in the Coil  $\rightleftharpoons$  Triple Helix Conversion of Collagen. *Eur. J. Biochem.* **1978**, *90*, 605-613.
10. Etzkorn, F. A.; Zhao, S., Stereospecific Phosphorylation by the Central Mitotic Kinase Cdk1-Cyclin B. *ACS Chem. Biol.* **2015**, *10*, 952-956.

11. Mayfield, J. E.; Fan, S.; Wei, S.; Zhang, M.; Li, B.; Ellington, A. D.; Etkorn, F. A.; Zhang, Y. J., Chemical Tools to Decipher Regulation of Phosphatases by Proline Isomerization on Eukaryotic RNA Polymerase II. *ACS Chem. Biol.* **2015**, *10*, 2405-2414.
12. Wang, X. J.; Xu, B.; Mullins, A. B.; Neiler, F. K.; Etkorn, F. A., Conformationally Locked Isostere of PhosphoSer-cis-Pro Inhibits Pin1 23-Fold Better than PhosphoSer-trans-Pro Isostere. *J. Am. Chem. Soc.* **2004**, *126*, 15533-15542.
13. Dai, N.; Wang, X. J.; Etkorn, F. A., The Effect of a Trans-Locked Gly-Pro Alkene Isostere on Collagen Triple Helix Stability. *J. Am. Chem. Soc.* **2008**, *130*, 5396-5397.
14. Dai, N.; Etkorn, F. A., Cis-Trans Proline Isomerization Effects on Collagen Triple-Helix Stability are Limited. *J. Am. Chem. Soc.* **2009**, *131*, 13728-13732.
15. Newberry, R. W.; Raines, R. T., The  $n \rightarrow \pi^*$  Interaction. *Acc. Chem. Res.* **2017**, *50*, 1838-1846.
16. Etkorn, F. A.; Ware, R. I.; Pester, A. M.; Troya, D., Conformational Analysis of  $n \rightarrow \pi^*$  Interactions in Collagen Triple Helix Models. *J. Phys. Chem. B* **2019**, *123*, 496-503.
17. Bürgi, H. B.; Dunitz, J. D.; Shefter, E., Geometrical Reaction Coordinates. II. Nucleophilic Addition to a Carbonyl Group. *J. Am. Chem. Soc.* **1973**, *95*, 5065-5067.
18. Choudhary, A.; Gandla, D.; Krow, G. R.; Raines, R. T., Nature of Amide Carbonyl-Carbonyl Interactions in Proteins. *J. Am. Chem. Soc.* **2009**, *131*, 7244-7246.
19. Newberry, R. W.; VanVeller, B.; Guzei, I. A.; Raines, R. T.,  $n \rightarrow \pi^*$  Interactions of Amides and Thioamides: Implications for Protein Stability. *J. Am. Chem. Soc.* **2013**, *135*, 7843-7846.
20. Worley, B.; Richard, G.; Harbison, G. S.; Powers, R.,  $^{13}\text{C}$  NMR Reveals No Evidence of  $n \rightarrow \pi^*$  Interactions in Proteins. *PLoS One* **2012**, *7*, e42075.
21. Rahim, A.; Saha, P.; Jha, K. K.; Sukumar, N.; Sarma, B. K., Reciprocal Carbonyl-Carbonyl Interactions in Small Molecules and Proteins. *Nat. Comm.* **2017**, *8*, 78.
22. Drouin, M.; Paquin, J., Recent Progress in the Racemic and Enantioselective Synthesis of Monofluoroalkene-Based Dipeptide Isosteres. *Beilstein J. Org. Chem.* **2017**, *13*, 2637-2658.
23. Tamamura, H.; Kobayakawa, T.; Ohashi, N., Chloroalkene Dipeptide Isosteres as Peptidomimetics. In *Mid-size Drugs Based on Peptides and Peptidomimetics*, Springer: Singapore, 2018; pp 17-47.
24. Bondi, A., van der Waals Volumes and Radii. *J. Phys. Chem.* **1964**, *68*, 441-451.
25. Abraham, R. J.; Ellison, S. L. R.; Schonholzer, P.; Thomas, W. A., A Theoretical and Crystallographic Study of the Geometries and Conformations of Fluoro-Olefins as Peptide Analogues. *Tetrahedron* **1986**, *42*, 2101-2110.

26. Pauling, L., The Nature of the Chemical Bond. IV. The Energy of Single Bonds and the Relative Electro negativity of Atoms. *J. Am. Chem. Soc.* **1932**, *54*, 3570-3582.
27. Kamer, K. J.; Choudhary, A.; Raines, R. T., Intimate Interactions with Carbonyl Groups: Dipole-Dipole or  $n \rightarrow \pi^*$ ? *J. Org. Chem.* **2013**, *78*, 2099-2103.
28. Jakobsche, C. E.; Choudhary, A.; Miller, S. J.; Raines, R. T.,  $n \rightarrow \pi^*$  Interaction and  $n(\pi)$  Pauli Repulsion Are Antagonistic for Protein Stability. *J. Am. Chem. Soc.* **2010**, *132*, 6651–6653.
29. Holmgren, S. K.; Taylor, K. M.; Bretscher, L. E.; Raines, R. T., Code for Collagen's Stability Deciphered. *Nature* **1998**, *392*, 666-7.
30. Shoulders, M. D.; Guzei, I. A.; Raines, R. T., 4-Chloroprolines: Synthesis, Conformational Analysis, and Effect on the Collagen Triple Helix. *Biopolymers* **2007**.
31. Improta, R.; Berisio, R.; Vitagliano, L., Contribution of Dipole-Dipole Interactions to The Stability of the Collagen Triple Helix. *Protein Sci.* **2008**, *17*, 955-961.
32. Shoulders, M. D.; Raines, R. T., Interstrand Dipole-Dipole Interactions Can Stabilize the Collagen Triple Helix. *J. Biol. Chem.* **2011**, *286*, 22905-22912.
33. Bella, J.; Eaton, M.; Brodsky, B.; Berman, H. M., Crystal and Molecular Structure of a Collagen-Like Peptide at 1.9 Å Resolution. *Science* **1994**, *226*, 75-81.
34. Schmidt, J. R.; Polik, W. F. *WebMO Enterprise*, version 17.0.012e; WebMO LLC: Holland, MI, USA, 2019.
35. Frisch, M. J.; Trucks, G. W.; Schlegel, H. B.; Scuseria, G. E.; Robb, M. A.; Cheeseman, J. R.; Scalmani, G.; Barone, V.; Mennucci, B.; Petersson, G. A., et al. *Gaussian 09*, Gaussian, Inc.: Wallingford, CT, 2009.
36. Kang, Y. K.; Park, H. S., Internal Rotation About the C–N Bond of Amides. *J. Mol. Str.: THEOCHEM* **2004**, *676*, 171-176.
37. Weinhold, F.; Landis, C., R., Natural Bond Orbitals and Extensions of Localized Bonding Concepts. *Chem. Educ. Res. Pract.* **2001**, *2*, 91-104.
38. The PyMOL Molecular Graphics System 2.0; Schrödinger, LLC.
39. Schrödinger Release 2021-3: Maestro, S., LLC, New York, NY, 2021.
40. Ramachandran, G. N.; Mitra, A. K., An Explanation for the Rare Occurrence of Cis Peptide Units in Proteins and Polypeptides. *J. Mol. Biol.* **1976**, *107*, 85–92.
41. Harris, T.; Chenoweth, D. M., Sterics and Stereoelectronics in Aza-Glycine: Impact of Aza-Glycine Preorganization in Triple Helical Collagen. *J. Am. Chem. Soc.* **2019**, *141*, 18021-18029.
42. von R. Schleyer, P.; West, R., Comparison of Covalently Bonded Electro-Negative Atoms

As Proton Acceptor Groups In Hydrogen Bonding. *J. Am. Chem. Soc.* **1959**, *81*, 3164-3165.

43. Mishra, S. K.; Suryaprakash, N., Intramolecular Hydrogen Bonding Involving Organic Fluorine: NMR Investigations Corroborated by DFT-Based Theoretical Calculations. *Molecules* **2017**, *22*, 423-467.

44. Gallo, E. A.; Gellman, S. H., N-H- $\pi$  Hydrogen Bonding in a Norbornenyl Diamide. *Tetrahedron Lett.* **1992**, *33*, 7485-7488.